HHS Public Access

Author manuscript

Nat Biotechnol. Author manuscript; available in PMC 2012 May 01.

Published in final edited form as:

Nat Biotechnol. ; 29(11): 1005–1010. doi:10.1038/nbt.1989.

Therapeutic siRNA silencing in inflammatory monocytes

Florian Leuschner[*,1], **Partha Dutta**[*,1], **Rostic Gorbatov**[1], **Tatiana I. Novobrantseva**[2], **Jessica Sullivan**[1], **Gabriel Courties**[1], **Kang Mi Lee**[3], **James I. Kim**[3], **James F. Markmann**[3], **Brett Marinelli**[1], **Peter Panizzi**[4], **Won Woo Lee**[5], **Yoshiko Iwamoto**[1], **Stuart Milstein**[2], **Hila Epstein-Barash**[2], **William Cantley**[2], **Jamie Wong**[2], **Virna Cortez-Retamozo**[1], **Andita Newton**[1], **Kevin Love**[6], **Peter Libby**[7], **Mikael J. Pittet**[1], **Filip K. Swirski**[1], **Victor Koteliansky**[2], **Robert Langer**[6,8,9], **Ralph Weissleder**[1,10], **Daniel G. Anderson**[6,8,9], and **Matthias Nahrendorf**[1]

[1]Center for Systems Biology, Massachusetts General Hospital and Harvard Medical School, Simches Research Building, 185 Cambridge St., Boston, MA 02114, USA

[2]Alnylam Pharmaceuticals, 300 3rd Street, Cambridge, MA 02142, USA

[3]Department of Surgery, MGH

[4]Department of Pharmacal Sciences, Harrison School of Pharmacy, Auburn University, Auburn, AL 36849, USA

[5]Department of Nuclear Medicine, Seoul National University Bundang Hospital, 166 Gumi-ro, Seongnam 463-707, Korea

[6]David H. Koch Institute for Integrative Cancer Research, Massachusetts Institute of Technology, 77 Massachusetts Avenue, Cambridge, MA, 02139, USA

[7]Cardiovascular Division, Department of Medicine, Brigham and Women's Hospital, Boston, MA

[8]Department of Chemical Engineering, MIT

[9]Division of Health Science Technology, MIT

[10]Department of Systems Biology, Harvard Medical School, Boston, MA

Abstract

Corresponding authors: Matthias Nahrendorf and Ralph Weissleder, Center for Systems Biology, 185 Cambridge Street, Boston, MA 02114, Tel: (617) 643-0500, Fax: (617) 643-6133, mnahrendorf@mgh.harvard.edu, rweissleder@mgh.harvard.edu.

*These authors contributed equally to this work

Contributions: F.L. and P.D. performed experiments, collected and analyzed the data, and contributed to writing the manuscript, R.G. did surgeries and performed experiments, T.I.N. designed experiments and siRNA screens, analyzed data and contributed to writing the manuscript; K.M.L. did islet transplantations and analyzed data, J.I.K., J.F.M., B.M., P.P., W.W.L., Y.I., V.C.R., A.N., W.C., J.W. performed experiments, imaging, collected, analyzed and discussed data, S.M., H.E.B., K.L. formulated siRNA nanoparticles, P.L., M.J.P., and F.K.S. conceived experiments and discussed strategy and results; V.K. R.L., R.W., D. A. and M.N. designed experiments, developed siRNA delivery technology and in vivo imaging strategies and systems, and reviewed, analyzed and discussed data. MN and RW wrote the manuscript which was edited and approved by all co-authors. M.N. developed and supervised the project.

Competing financial interest: T.I.N., S.M., H.E.B., W.C., J.W. and V.K. are Alnylam Pharmaceuticals employees; K.L., R.L., and D.G.A. receive funding from Alnylam Pharmaceuticals. R.L. and D.G.A. are consultants with Alnylam. The other authors declare no competing financial interests.

Inflammatory monocytes -- but not the non-inflammatory subset -- depend on the chemokine receptor CCR2 for distribution to injured tissue and stimulate disease progression. Precise therapeutic targeting of this inflammatory monocyte subset could spare innate immunity's essential functions for maintenance of homeostasis and thus limit unwanted effects. Here we developed siRNA nanoparticles targeting CCR2 expression in inflammatory monocytes. We identified an optimized lipid nanoparticle and silencing siRNA sequence that when administered systemically, had rapid blood clearance, accumulated in spleen and bone marrow and showed high cellular localization of fluorescently tagged siRNA inside monocytes. Efficient degradation of CCR2 mRNA in monocytes prevented their accumulation in sites of inflammation. Specifically, the treatment attenuated their number in atherosclerotic plaques, reduced infarct size following coronary artery occlusion, prolonged normoglycemia in diabetic mice after pancreatic islet transplantation and resulted in reduced tumor volumes and lower numbers of tumor-associated macrophages. Taken together, siRNA nanoparticle-mediated CCR2 gene silencing in leukocytes selectively modulates functions of innate immune cell subtypes and may allow for the development of specific anti-inflammatory therapy.

Introduction

Our understanding of the innate immune system's role in homeostasis and disease has considerably expanded over the last decades. The cellular arm, in particular monocytes and their lineage descendant macrophages, participate critically in inflammatory activity in major diseases. The production, recruitment and differentiation of monocytes, their subsets and their progeny have been studied in detail[1-3]; however, this knowledge has not yet resulted in effective clinical therapies. A major hurdle for translation is the multitude of protective functions of innate immune cells, many of which are too important for survival to compromise. A possible solution to this problem is a therapy that “surgically” and temporarily targets cellular subsets with compromising disease activity while leaving other classes of cells undisturbed, so the latter can maintain homeostasis, foster healing, resolve inflammation and defend against infection. While such therapeutic precision has remained elusive, the emerging differential roles of monocyte and macrophage subsets make this goal more attainable.

Inflammatory monocytes (Ly-6C^{high} in the mouse, CD14^{+}CD16^{-} in human)[3] give rise to classical macrophages and promote inflammatory disease activity. While essential early responders, their excessive or prolonged recruitment hinders resolution of inflammation and propagates disease progression. The recruitment of inflammatory monocytes depends on the chemokine/chemokine receptor pair MCP-1/CCR2, distinct from the non-inflammatory monocyte subset which depends on fractalkine/CX3CR1[1]. CCR2 also mediates egress of monocytes from the bone marrow[4]. Accordingly, genetic deletion of either MCP-1 or CCR2 results in profound reduction of inflammation in various disease models[5-10]. Therapeutic targeting of CCR2 could thus limit harmful functions of innate immunity while leaving non-inflammatory monocytes, alternatively activated macrophages, antigen-presenting cells and other tissue residents unaffected. Small molecules and neutralizing antibodies targeting the MCP-1/CCR2 axis are being investigated but often lack specificity or *in vivo* efficacy[1].

Small interference RNA (siRNA) technology shows promise to attenuate production of specific target proteins *in vivo* by degradation of mRNA (e.g.[11,12]). While siRNA delivery has been the focus of considerable work, the development of formulations capable of efficacious systemic delivery to immune cells with clinically suitable delivery materials has been challenging[13]. Recent advances in siRNA design and chemistry now allow identification of specific, highly potent sequences with nuclease stability and reduced immunostimulation[14], which we here combine with biocompatible nanoparticle delivery vehicles[15]. We hypothesized that emerging monocyte-targeting siRNA nanomaterials could silence CCR2 mRNA in the inflammatory monocyte subset to selectively inhibit migration (and consequently adverse function) of these cells and their progeny (Supplementary Fig. 1). Dynamic optical tomography revealed that nanoparticle-encapsulated, fluorescently tagged siRNA rapidly redistributed from the blood pool to the spleen and bone marrow. Knock down of CCR2 in monocytes was confirmed at the mRNA, protein and functional levels. We then tested this therapeutic approach in mouse atherosclerosis, myocardial infarction, pancreatic islet transplantation in diabetes, and cancer. Treatment with clinically feasible doses of siRNA substantially reduced regional recruitment of inflammatory monocytes and attenuated disease progression in these disease models.

Results

siRNA distribution

The siRNA carrier used in this study was identified in high-throughput *in vitro* screens of several hundred compounds, resulting in development of a 70-80 nm lipid-like particle with efficient cell delivery and knock down[15]. The nanoparticle was formulated using C12-200 lipid, disteroylphosphatidyl choline, cholesterol, PEG-DMG and siRNA in a spontaneous vesicle formation procedure. The specific siRNA sequence against CCR2 (siCCR2) was identified by *in vitro* screening from 31 candidate sequences (Supplementary Fig. 2), all chemically modified to minimize off-target effects. The best duplex with the sequence of 5′-uGcuAAAcGucucuGcAAAdTsdT-3′ (sense), 5′- UUUGcAGAGACGUUuAGcAdTsdT -3′ (anti-sense) was selected for scale up, formulation and subsequent nanoparticle encapsulation. The final lipid:siRNA weight ratio of the nanoparticle was 12:1 with an siRNA entrapment efficiency of 95%.

We covalently labeled siRNA with a near infrared fluorochrome to follow its *in vivo* distribution after intravenous injection with dynamic fluorescence imaging. Mice were positioned inside the Fluorescence Molecular Tomography (FMT) scanner, and data were acquired serially for up to 24 hours. siRNA concentration was determined every 5 minutes. Key organs were identified in co-registered X-ray computed tomography (CT). Immediately after injection, strong fluorescence signal localized in the cardiac region, reflecting the presence of siRNA in the blood pool (Fig. 1a, arrow). This signal was fitted over time resulting in an siRNA blood half-life of 8.1 minutes (Fig. 1a). Interestingly, the spleen showed the highest fluorescence per gram of tissue in the entire body, with a peak fluorescence of 391±63 pmol/g tissue (Fig. 1a, circle). There was also considerable accumulation in the bone marrow, while no siRNA was detected in the lung (3±4 pmol/g). Dynamic imaging identified that the siRNA was excreted via the hepato-biliary route (Fig.

1a). *Ex vivo* fluorescence reflectance imaging corroborated these findings (Supplementary Fig. 3).

We next studied the intra-parenchymal siRNA distribution in the spleen by fluorescence microscopy. Most of the siRNA related fluorescence was found in cells residing in the red pulp. Spectrally resolved co-staining for CD11b co-localized this myeloid marker with siRNA in cells that formed the typical splenic reservoir monocyte clusters[16] (Fig. 1b). We also detected uptake in Kupffer cells (Supplementary Fig. 4). Flow cytometric analysis further refined the uptake profile in cells in the bone marrow and spleen, and in circulating leukocytes. While lymphocytes showed comparatively low uptake, we detected strong signal in neutrophils, Ly-6C^{high} and Ly-6C^{low} monocytes, dendritic cells and macrophages (Fig. 1c). The highest uptake was seen in splenic Ly-6C^{high} monocytes (Fig. 1d).

In vivo silencing in Ly-6C^{high} monocytes

Recent work described a large monocyte reservoir in the spleen which dispatches these cells to sites of local inflammation[16]. Systemic treatment with nanoparticle-encapsulated siCCR2 resulted in a significant reduction of CCR2 mRNA in Ly-6C^{high} monocytes isolated from this population (Fig. 2a). A RACE assay in splenic monocytes isolated after intravenous injection confirmed the RNAi mechanism by detecting specific mRNA cleavage products (Supplementary Fig. 5). Cleavage of CCR2 mRNA translated into lower protein levels by Western blot (Fig. 2b, Supplementary Fig. 6) and flow cytometric staining of CCR2 protein on Ly-6C^{high} monocytes (Fig. 2c). The migratory capacity of Ly-6C^{high} monocytes towards MCP-1 was drastically reduced from 144±31 to 2±2 migrated cells (Fig. 2d).

Silencing of CCR2 reduces myocardial infarct size

Myocardial infarction elicits a strong inflammatory response and profound recruitment of innate immune cells, including inflammatory splenic reservoir monocytes[16]. The magnitude of inflammation influences infarct size and the degree of post-MI heart failure[17]. Using flow cytometry analysis of digested myocardium that underwent ischemia followed by reperfusion, we found a marked reduction of monocytes and macrophages in the hearts of mice that had been injected with siCCR2 (control siRNA treatment, 16,950±9,470 cells per mg infarct tissue; siCCR2 treatment, 5,158±2,201; Fig. 3a,b). The treatment lowered the number of inflammatory Ly-6C^{high} monocytes by 71% (Fig. 3a,b). The infarct-to-area-at-risk ratio, which signifies the benefit of a treatment acutely after myocardial ischemia, was reduced by 34% in siCCR2 injected mice (Fig. 3c,d). Splenectomy experiments confirmed that the splenic monocyte reservoir is a major target of siCCR2 treatment in acute inflammation (Fig. 3e-g). When treatment was started 1 hour after injury, therapeutic effects were preserved (Supplementary Fig. 7). A head-to-head comparison to small molecule inhibitors of CCR2 showed superior efficacy of therapeutic silencing (Supplementary Fig. 8).

Silencing of CCR2 reduces inflammatory atherosclerosis

Increased invasion of Ly-6C^{high} monocytes critically promotes progression and complication of atherosclerosis[18,19] while germline deletion of CCR2[6] or MCP-1[5] attenuates the disease. A 3 week siCCR2 therapy in apoE$^{-/-}$ mice with established

atherosclerosis reduced the monocyte/macrophage number in atherosclerotic plaques by 82% (Fig. 4a,b). Monocyte subset analysis showed a marked reduction of inflammatory Ly-6C^{high} monocytes (7,188 ± 3,388 versus 2,281 ± 1581). Immunohistochemical staining for CD11b indicated a 46% reduced presence of myeloid cells, and a 38% reduction of lesion size in the aortic root (Fig. 4c).

Silencing of CCR2 prolongs islet graft survival

Pancreatic islet transplantation is a treatment option for patients with type 1 diabetes; however, allograft rejection is a major hurdle to its clinical use[20]. Ly-6C^{high} monocytes are recruited in transplant rejection[21], and monocytes can differentiate into highly active antigen-presenting cells[3]. Therefore, we investigated the effect of siCCR2 treatment in pancreatic islet transplantation in mice with streptozotocin-induced diabetes. Intravenous injection of nanoparticle-encapsulated siCCR2 significantly prolonged the normoglycemic period and by association islet graft function (Fig. 5a). Graft-dependent normoglycemia in siCCR2 treated mice was established by nephrectomy, which removed the grafted islets and returned mice to a diabetic state. Histology of the grafted islets confirmed that these were rejected in control groups, but not in euglycemic mice treated with siCCR2 (Fig. 5b,c)

Silencing of CCR2 reduces tumor size and TAM

The host immune system plays an increasingly recognized role in cancer progression, including tumor vascularisation, growth, metastasis and resistance to chemotherapy[22-25]. Inflammatory monocytes contribute substantially to the host response by differentiation into tumor-associated macrophages (TAM)[26], and the number of TAM inversely correlates with survival in patients with lymphoma[27]. Accordingly, we investigated the effect of siCCR2 therapy in mice after implantation of lymphoma EL4 cells. Treatment was initiated when a tumor mass was palpable, which occurred 6 to 10 days after inoculation. Starting on day 14 after tumor implantation, tumor size was reduced in siCCR2 treated mice (Supplementary Fig. 9). Computed tomography showed that tumor volume was significantly reduced after siCCR2 injections (279±144mm^3 versus 590±221 mm^3, Fig. 6a). Flow cytometric analysis of tumors showed a 54% reduction of tumor-associated macrophages in mice treated with siCCR2 (Fig. 6b). Histological analysis confirmed reduced numbers of CD11b$^+$ cells (Fig. 6c) and showed that the expression of VEGF and the number of microvessels was reduced after treatment with siCCR2 (Fig. 6d,e). In a second cancer model of colorectal CT26 tumors we found a 75% reduction of tumor associated macrophages (Supplementary Fig. 10). Taken together, treatment with siCCR2 reduced the number of TAMs and tumor size, however; future experiments will have to show impact of this therapy at later disease stages and in conjunction with chemotherapy.

Cellular specificity and other gene targets

We were interested to better understand the specificity of siCCR2 treatment, and therefore investigated reduction of other leukocytes in cancerous lesions. As expected, we found that silencing of CCR2 primarily reduced the number of inflammatory monocytes, which depend on this receptor for recruitment. Other myeloid cells and lymphocytes were affected less (Supplementary Fig. 11). However, silencing of the pan-leukocyte marker CD45 was also

possible in splenic macrophages, Ly-6C^{low} monocytes and dendritic cells (Supplementary Fig. 12), implying that the approach is broadly applicable for silencing genes in those cells.

Discussion

The controlled recruitment of monocytes is an essential feature of host defense, but excessive or prolonged recruitment of the inflammatory monocyte subset is harmful as these cells are mediators of tissue destruction. Here we harnessed RNA interference to silence expression of the monocytic chemokine receptor CCR2, which is responsible for the migration of the inflammatory monocyte subset. Migration of monocytes towards MCP-1 is severely attenuated in heterozygous CCR2 deficient mice[28], making CCR2 an efficient silencing target since even intermediate protein levels translate into impaired migratory capacity of Ly-6C^{high} monocytes.

The motivation for targeting CCR2 in monocytes in this study was based on three major observations: i) the striking phenotype of CCR2$^{-/-}$ and MCP-1$^{-/-}$ mice[1,5-10,29,30]; ii) prior work linking monocyte subsets to distinct functions in disease and healing[2,3,17,25,31] and iii) the ease by which monocytes can be targeted via their phagocytic activity[32]. Based on recent advances in siRNA formulation designs, we show by dynamic FMT imaging and flow cytometry that intravenously injected nanoparticles distributed siRNA to immune cells in the blood, bone marrow and spleen, resulting in efficient and specific knock down of CCR2. Consequently, fewer inflammatory monocytes migrated to the site of inflammation and disease severity was attenuated in multiple models investigated. Because we target a recruitment mechanism, sessile immune cells remain largely unaffected.

The effects of siCCR2 treatment on splenic reservoir monocytes proved particularly intriguing. Study of acute myocardial infarction firmly established the dominant role of this emergency reservoir, as more than half of the monocytes recruited to the infarct originate from the spleen[16]. Splenectomy and siCCR2 treatment had no additive effects on recruitment to the infarct, indicating that the splenic monocyte population is a major target of siCCR2 therapy, and potentially for any anti-inflammatory strategy focusing on monocytes. The role of splenic monocytes is less well understood in chronic inflammation, and future studies will decipher if lesional foam cells in atherosclerosis and tumor-associated macrophages derive from the splenic monocyte pool. Observed treatment effects in atherosclerosis and cancer in our study likely also result from CCR2 silencing in bone marrow or circulating monocytes.

Our approach is distinct from previous work on gene silencing in leukocytes on several levels. We targeted a monocyte gene that drives recruitment of a cells. Interruption of cell migration may be particularly efficient, because it removes a cell population from the inflammatory site rather than neutralizing a single gene product. To our knowledge, this is the first demonstration of siRNA delivery to the inflammatory monocyte subset. Silencing CCR2 provides cellular specificity for this emerging therapeutic target. A previous study described silencing after oral administration of yeast-based glucan particles. These micrometer sized particles were reported as taken up by macrophages in the intestine through a glucan-receptor mediated pathway[11]. A smaller liposome that is comparable in

size to the nanoparticle used in our study was formed from phospholipids and featured a monoclonal antibody against integrins as a targeting moiety[12]. The lipidoid nanoparticle preparation used in our study consists of chemically defined entities and comes with significant manufacturing advantages[13], which enhance chances of its clinical use for anti-inflammatory therapy. Structurally related delivery materials have been used successfully for silencing in the liver by independent research groups in several species, with potent knock down at doses as low as 0.01mg/kg[33].

When compared to conventional anti-inflammatory therapy (e.g. steroids, cyclooxygenase-2 inhibitors, methotrexate), silencing CCR2 is set apart by its cellular specificity. Most clinically approved drugs may have molecular specificity but broadly target cells in tissues they distribute to, including cells that should be spared to avoid unwanted side effects. For example, steroids have been tested in patients with myocardial infarction with disastrous outcomes[34], and their side effects (fluid retention, diabetes) make them an unlikely candidate for treating cardiovascular disease. Other potent immunosuppressive drugs such as methotrexate, used for treatment of rheumatoid arthritis, also lack cellular specificity. Therefore, while these drugs suppress inflammation, they also diminish protective functions of the immune system which are involved in the resolution of inflammation, wound healing and defense against infection. In general, delivery of drugs by nanoparticles can increase their concentration at the site of action[35], which may partially explain the advantage in efficiency when we compared siCCR2 treatment with small molecule CCR2 inhibitors.

The efficient delivery of siRNA to immune cells provides an avenue to translate the vast knowledge base gained from germline inactivation of genes involved in immunity. While we have concentrated on CCR2 in this study, it is logical to extend the approach to other targets in innate immune cells, for instance proteins involved in proliferation, maturation, differentiation, antigen presentation, such as transcription factors and cytokines. The ability to silence CD45 in other myeloid cells suggests that generalization of the approach is feasible. One particularly appealing aspect of siRNA delivery is the ability to co-silence multiple targets. While we have shown the ubiquitous (and surprising) efficacy of CCR2 siRNA in cardiovascular disease, cancer and transplant rejection, there are likely even more diseases that could benefit. In sum, this study describes the merging of in vivo RNA interference with recent insight into monocyte biology, opening a new translational avenue to approach the many diseases driven by recruitment of these cells.

Methods

See Supplementary Methods for a detailed description of mouse models, imaging, molecular biology, immunohistology and statistical analysis. All experiemnts were approved by the Subcommittee on Animal Research Care at Massachusetts General Hospital.

Synthesis and *in vitro* screening of siRNAs

31 siRNAs with the lowest predicted off-target potentials and 100% homology with mouse CCR2 gene sequence NM_009915.2 were selected for synthesis and screening. Single-strand RNAs were produced at Alnylam Pharmaceuticals as previously described, annealed and used as duplexes[36]. Mouse macrophage line J774A.1 cells were transfected with siRNA

by using Lipofectamine RNAiMAX reagent according to the manufacturer's protocols at 0.1nM and 10nM concentrations. CCR2 mRNA levels were quantified 24h post transfection by Q-PCR and normalized to GAPDH mRNA. Duplexes showing best knock-down at both concentrations (marked with arrows in Supplemental Figure 2) were selected for 12 point dose response ranging from 10nM down to 0.01pM to determine IC_{50} value for these siRNA duplexes. The best duplex with the sequence of 5′-uGcuAAAcGucucuGcAAAdTsdT-3′ (sense), 5′- UUUGcAGAGACGUUuAGcAdTsdT -3′ (anti-sense) was selected for scaling up, formulating and subsequent in vivo work. Small case represents 2'OMe modified residues. For silencing CD45, we used a duplex with the following sequence: 5′-cuGGcuGAAuuucAGAGcAdTsdT-3′ (sense), 5′- UGCUCUGAAAUUcAGCcAGdTsdT-3′ (antisense) as published previously[37].

siRNA formulation into lipid nanoparticles

Nanoparticles were prepared with the cationic lipid C12-200,[15] disteroylphosphatidyl choline, cholesterol, and PEG–DMG using a spontaneous vesicle formation formulation procedure. Lipids were dissolved in 90% ethanol solution and mixed with siRNA solution (25 mM citrate, pH 3 ratio) at fixed speed (1:1 ratio) and diluted immediately with PBS to final 25% ethanol. The ethanol was then removed and the external buffer replaced with PBS (155 mM NaCl, 3 mM Na2HPO4, 1 mM KH2PO4, pH 7.5) by dialysis. The particles had a component molar ratio of ∼50/10/38.5/1.5 (C12-200/disteroylphosphatidyl choline/ cholesterol/PEG–DMG). The final lipid:siRNA weight ratio was ∼7:1. Particle size and zeta potential were determined using a Malvern Zetasizer NanoZS (Malvern, UK). siRNA content was determined by ion exchange HPLC (Agilent) assay using DNAPac Pa200 column (Dionex Corporation Dionex, 260nm, 55°C run at 2mL/min). siRNA entrapment efficiency was determined by the Quant-iT RiboGreen RNA assay (Invitrogen, Carlsbad, CA)[38]. Briefly, siRNA entrapment was determined by comparing the signal of the RNA binding dye RiboGreen in formulation samples in the absence and presence of the detergent Triton-X100. In the absence of detergent, signal comes from accessible (unentrapped) siRNA only. In the presence of detergent, signal comes from total siRNA. In all preparations used the encapsulation was above 82%. The polydispersity index of the final formulation was 0.036-0.037.

Dynamic FMT-CT imaging of siRNA biodistribution

FMT-CT imaging was used to evaluate the time-resolved biodistribution of lipid nanoparticle siRNA. This quantitative imaging technique combines non-invasive whole body fluorescent tomography (determining tissue concentration of AF647-coupled siRNA) with high resolution CT imaging. To minimize absorbance of photons by fur nude mice were used for this study, which received a non-fluorescent diet for a week prior to imaging. After placement of mice into a multimodal imaging cartridge which provides fiducials detected by both modalities for image fusion, contrast-enhanced microCT (Inveon, Siemens) was followed by dynamic FMT imaging on an FMT-2500 system (PerkinElmer). Anesthesia used 1.5 % Isoflurane (O2 2L/min) with a gas delivery system integrated into the multimodal imaging cartridge. After CT imaging, mice were transferred while in the multimodal imaging cartridge and positioned in the FMT scanner with a tail vein in place. Then, a bolus of nanoparticle-encapsulated AF647-coupled siRNA was injected at a dose of

1 mg/kg, and mice were imaged every 5 minutes for 2 hours, and then at 4hrs, 6hrs, 8hrs, and 24hrs post-injection. FMT imaging used excitation/emission wavelengths of 635 and 655nm, respectively. 30 frontal slices of 0.5 mm thickness in z-direction, with an in-plane resolution of at least 1×1 mm were acquired.

Post-processing of FMT data sets was done by using a normalized Born forward equation to calculate fluorochrome concentration expressed in nM fluorescence per voxel. The 3D dataset was reconstructed for the entire mouse. Based on CT information, volumes of interest were defined in respective organs. To co-register FMT and CT images, DICOM-converted data were imported into OsiriX (The OsiriX foundation, Geneva, Switzerland). Fiducials on the imaging cartridge were visualized and tagged in FMT and CT images with point markers to define their location in 3D. This allows point-based registration of FMT data to CT coordinates as described before[39]. Fluorescence measurements in volumes of interest were normalized to weight using average organ weights and expressed as fluorescence per gram tissue.

Supplementary Material

Refer to Web version on PubMed Central for supplementary material.

Acknowledgments

The authors thank Michael Warring and the Ragon Institute (MGH) for cell sorting, the CSB Mouse Imaging Program (Peter Waterman, Brena Sena), Dr. Brian Bettencourt for designing initial sets of siRNA. We acknowledge the small, medium and large scale RNA synthesis groups at Alnylam as well as analytical, duplex annealing and QC groups for synthesizing and characterizing RNAs. This work was funded in part by grants from the National Institute of Health R01-HL096576, R01-HL095629 (M.N.); R01-EB006432, T32-CA79443, U24-CA92782, P50-CA86355, HHSN268201000044C (R.W.); R01-CA132091, R01-CA115527, R37-EB000244 (R.L.); Deutsche Herzstiftung (F.L.); the SNUBH Research Fund 02-2007-013 (W.W.L.).

References

1. Charo IF, Ransohoff RM. The many roles of chemokines and chemokine receptors in inflammation. N Engl J Med. 2006; 354:610–621. [PubMed: 16467548]
2. Gordon S, Taylor PR. Monocyte and macrophage heterogeneity. Nat Rev Immunol. 2005; 5:953–964. [PubMed: 16322748]
3. Geissmann F, et al. Development of monocytes, macrophages, and dendritic cells. Science. 2010; 327:656–661. [PubMed: 20133564]
4. Serbina NV, Pamer EG. Monocyte emigration from bone marrow during bacterial infection requires signals mediated by chemokine receptor CCR2. Nat Immunol. 2006; 7:311–317. [PubMed: 16462739]
5. Gu L, et al. Absence of monocyte chemoattractant protein-1 reduces atherosclerosis in low density lipoprotein receptor-deficient mice. Mol Cell. 1998; 2:275–281. [PubMed: 9734366]
6. Boring L, Gosling J, Cleary M, Charo IF. Decreased lesion formation in CCR2-/- mice reveals a role for chemokines in the initiation of atherosclerosis. Nature. 1998; 394:894–897. [PubMed: 9732872]
7. Dewald O, et al. CCL2/Monocyte Chemoattractant Protein-1 regulates inflammatory responses critical to healing myocardial infarcts. Circ Res. 2005; 96:881–889. [PubMed: 15774854]
8. Kaikita K, et al. Targeted deletion of CC chemokine receptor 2 attenuates left ventricular remodeling after experimental myocardial infarction. Am J Pathol. 2004; 165:439–447. [PubMed: 15277218]

9. Abdi R, et al. Differential role of CCR2 in islet and heart allograft rejection: tissue specificity of chemokine/chemokine receptor function in vivo. J Immunol. 2004; 172:767–775. [PubMed: 14707046]
10. Lu X, Kang Y. Chemokine (C-C motif) ligand 2 engages CCR2+ stromal cells of monocytic origin to promote breast cancer metastasis to lung and bone. J Biol Chem. 2009; 284:29087–29096. [PubMed: 19720836]
11. Aouadi M, et al. Orally delivered siRNA targeting macrophage Map4k4 suppresses systemic inflammation. Nature. 2009; 458:1180–1184. [PubMed: 19407801]
12. Peer D, Park EJ, Morishita Y, Carman CV, Shimaoka M. Systemic leukocyte-directed siRNA delivery revealing cyclin D1 as an anti-inflammatory target. Science. 2008; 319:627–630. [PubMed: 18239128]
13. Whitehead KA, Langer R, Anderson DG. Knocking down barriers: advances in siRNA delivery. Nat Rev Drug Discov. 2009; 8:129–138. [PubMed: 19180106]
14. Judge AD, et al. Confirming the RNAi-mediated mechanism of action of siRNA-based cancer therapeutics in mice. J Clin Invest. 2009; 119:661–673. [PubMed: 19229107]
15. Love KT, et al. Lipid-like materials for low-dose, in vivo gene silencing. Proc Natl Acad Sci U S A. 2010; 107:1864–1869. [PubMed: 20080679]
16. Swirski FK, et al. Identification of splenic reservoir monocytes and their deployment to inflammatory sites. Science. 2009; 325:612–616. [PubMed: 19644120]
17. Nahrendorf M, Pittet MJ, Swirski FK. Monocytes: protagonists of infarct inflammation and repair after myocardial infarction. Circulation. 2010; 121:2437–2445. [PubMed: 20530020]
18. Swirski FK, et al. Ly-6Chi monocytes dominate hypercholesterolemia-associated monocytosis and give rise to macrophages in atheromata. J Clin Invest. 2007; 117:195–205. [PubMed: 17200719]
19. Libby P. Inflammation in atherosclerosis. Nature. 2002; 420:868–874. [PubMed: 12490960]
20. Robertson RP. Islet transplantation as a treatment for diabetes - a work in progress. N Engl J Med. 2004; 350:694–705. [PubMed: 14960745]
21. Swirski FK, et al. Myeloperoxidase-rich Ly-6C+ myeloid cells infiltrate allografts and contribute to an imaging signature of organ rejection in mice. J Clin Invest. 2010; 120:2627–2634. [PubMed: 20577051]
22. Grivennikov SI, Greten FR, Karin M. Immunity, inflammation, and cancer. Cell. 2010; 140:883–899. [PubMed: 20303878]
23. Qian BZ, Pollard JW. Macrophage diversity enhances tumor progression and metastasis. Cell. 2010; 141:39–51. [PubMed: 20371344]
24. De Palma M, Lewis CE. Cancer: Macrophages limit chemotherapy. Nature. 2011; 472:303–304. [PubMed: 21512566]
25. Qian BZ, et al. CCL2 recruits inflammatory monocytes to facilitate breast-tumour metastasis. Nature. 2011; 475:222–225. [PubMed: 21654748]
26. Movahedi K, et al. Different tumor microenvironments contain functionally distinct subsets of macrophages derived from Ly6C(high) monocytes. Cancer Res. 2010; 70:5728–5739. [PubMed: 20570887]
27. Steidl C, et al. Tumor-associated macrophages and survival in classic Hodgkin's lymphoma. N Engl J Med. 2010; 362:875–885. [PubMed: 20220182]
28. El Khoury J, et al. Ccr2 deficiency impairs microglial accumulation and accelerates progression of Alzheimer-like disease. Nat Med. 2007; 13:432–438. [PubMed: 17351623]
29. Hart KM, Bak SP, Alonso A, Berwin B. Phenotypic and functional delineation of murine CX(3)CR1 monocyte-derived cells in ovarian cancer. Neoplasia. 2009; 11:564–73. [PubMed: 19484145]
30. Pahler JC, et al. Plasticity in tumor-promoting inflammation: impairment of macrophage recruitment evokes a compensatory neutrophil response. Neoplasia. 2008; 10:329–340. [PubMed: 18392134]
31. Nahrendorf M, et al. The healing myocardium sequentially mobilizes two monocyte subsets with divergent and complementary functions. J Exp Med. 2007; 204:3037–3047. [PubMed: 18025128]

32. Weissleder R, Pittet MJ. Imaging in the era of molecular oncology. Nature. 2008; 452:580–589. [PubMed: 18385732]
33. Vaishnaw AK, et al. A status report on RNAi therapeutics. Silence. 2010; 1:14. [PubMed: 20615220]
34. Roberts R, DeMello V, Sobel BE. Deleterious effects of methylprednisolone in patients with myocardial infarction. Circulation. 1976; 53:I204–6. [PubMed: 1253361]
35. Buxton DB. Nanotechnology research support at the national heart, lung, and blood institute. Circ Res. 2011; 109:250–254. [PubMed: 21778434]
36. Frank-Kamenetsky M, et al. Therapeutic RNAi targeting PCSK9 acutely lowers plasma cholesterol in rodents and LDL cholesterol in nonhuman primates. Proc Natl Acad Sci U S A. 2008; 105:11915–11920. [PubMed: 18695239]
37. Akinc A, et al. A combinatorial library of lipid-like materials for delivery of RNAi therapeutics. Nat Biotechnol. 2008; 26:561–569. [PubMed: 18438401]
38. Heyes J, Palmer L, Bremner K, MacLachlan I. Cationic lipid saturation influences intracellular delivery of encapsulated nucleic acids. J Control Release. 2005; 107:276–287. [PubMed: 16054724]
39. Nahrendorf M, et al. Hybrid PET-optical imaging using targeted probes. Proc Natl Acad Sci U S A. 2010; 107:7910–7915. [PubMed: 20385821]

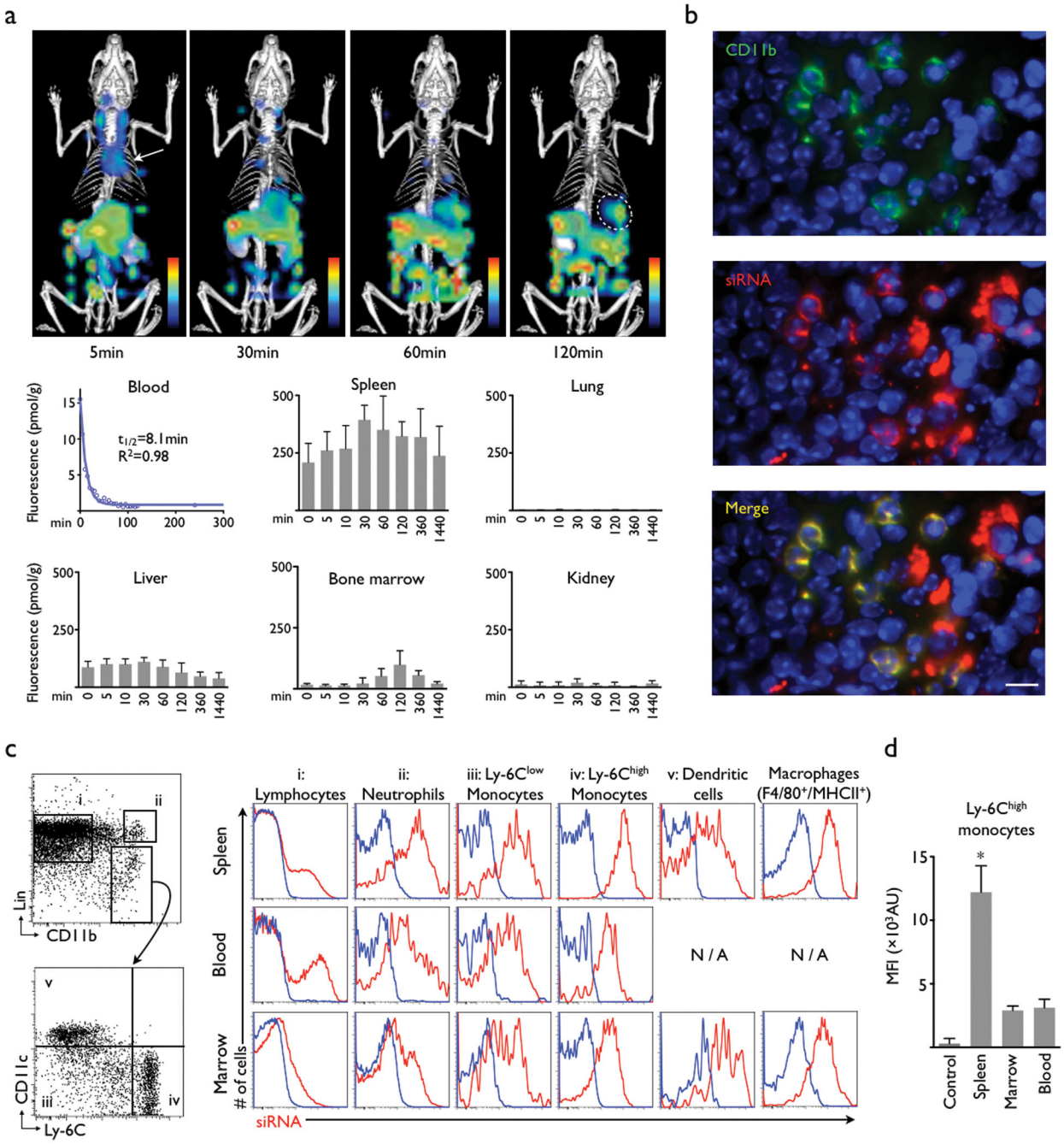

Figure 1. Nanoparticle-encapsulated siRNA distributes to leukocytes

(a) Dynamic FMT-CT biodistribution imaging of siRNA shows major uptake in the spleen (circle). The material is rapidly cleared from the blood pool (arrow) and excreted via the hepato-biliary route into bowel (n = 5). (b) Immunofluorescence microscopy of the splenic red pulp shows colocalization of siRNA (red), CD11b expression (green). The scale bar indicates 20μm. (c) Profiling by flow cytometry reveals strong uptake of siRNA into cells of the mononuclear phagocyte system in the bone marrow, blood and the spleen. Representative dot-plots on the left illustrate the gating strategy (lin: lineage markers).

Histograms on the right illustrate the uptake of siRNA (red) in the respective cells (columns) and organs (rows). Blue indicates control fluorescence in cells harvested from non-injected mice. (d) Comparison of siRNA content in Ly-6C^{high} monocytes retrieved from different organs (n = 3 mice per group). Mean ± SD, * $P < 0.05$.

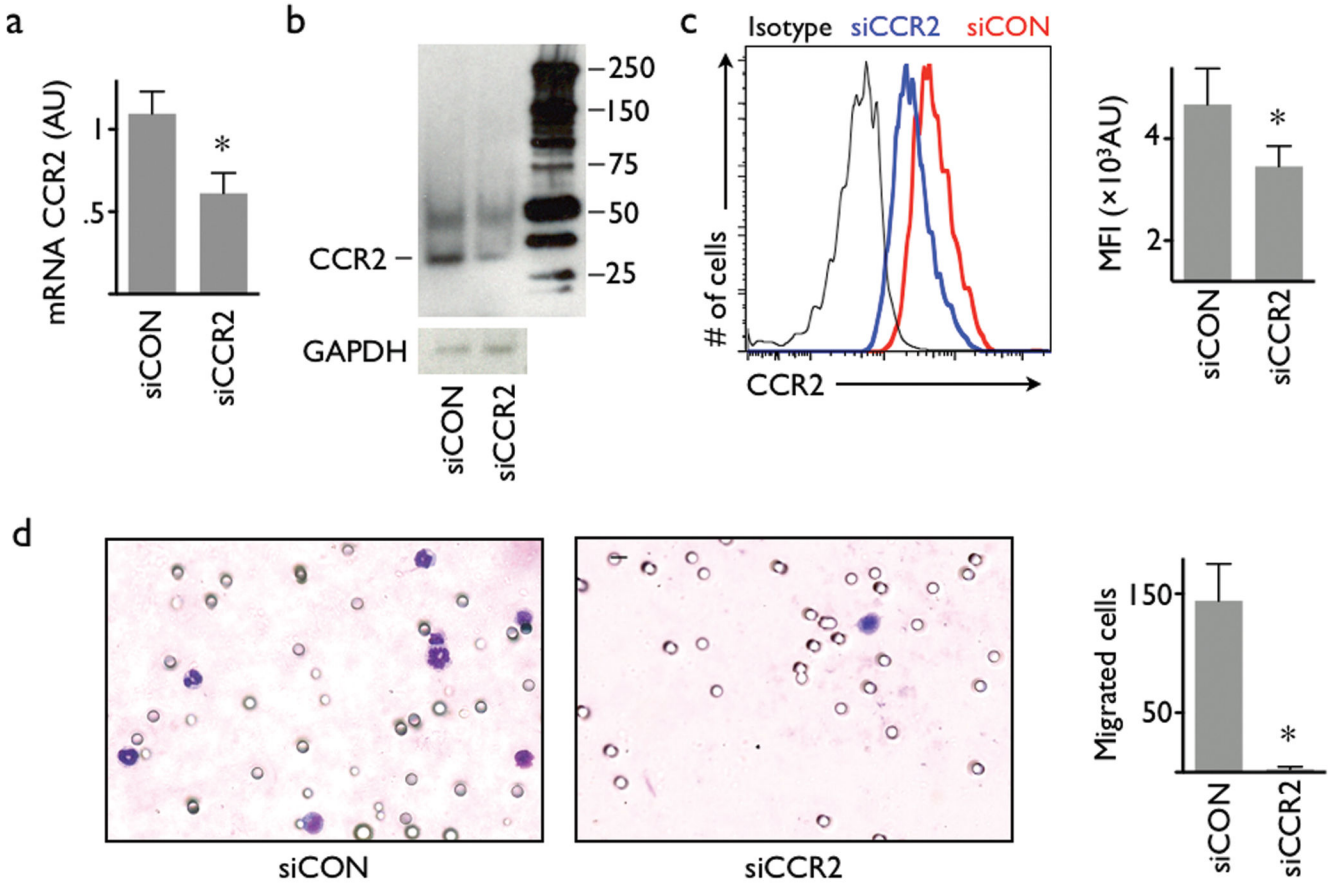

Figure 2. Intravenous injection of nanoparticle-encapsulated siRNA results in knock down in monocytes

(a) PCR analysis of FACS-sorted splenic Ly-6C^{high} monocytes after intravenous administration of nanoparticle-encapsulated siRNA targeting CCR2 (siCCR2). siCON: control siRNA treatment. n = 3 per group. (b) Western blot of Ly-6C^{high} monocytes isolated from the spleen of mice that were either treated with siCCR2 or control. The reduced band in the siCCR2 lane confirms a lower expression of CCR2 receptor protein in splenic monocytes after intravenous treatment (experiment was done in triplicate, representative blot is cropped. The full length blot is presented in Supplementary Figure 6). (c) FACS analysis of CCR2 protein on splenic Ly-6C^{high} monocytes. Representative histogram shows isotype antibody staining (black), control treatment (red) and siCCR2 treatment (blue). Bar graph of mean fluorescent intensity (MFI, y axis starts at mean fluorescence intensity of the isotype control; n = 6 per group). (d) Migration assay of sorted Ly-6C^{high} monocytes using MCP-1 as chemoattractant. Cells were harvested from mice injected with either siCCR2 or control siRNA (n = 3 per group). Stained membranes on the left, bar graph shows enumeration of migrated cells. Mean ± SD, * $P < 0.05$.

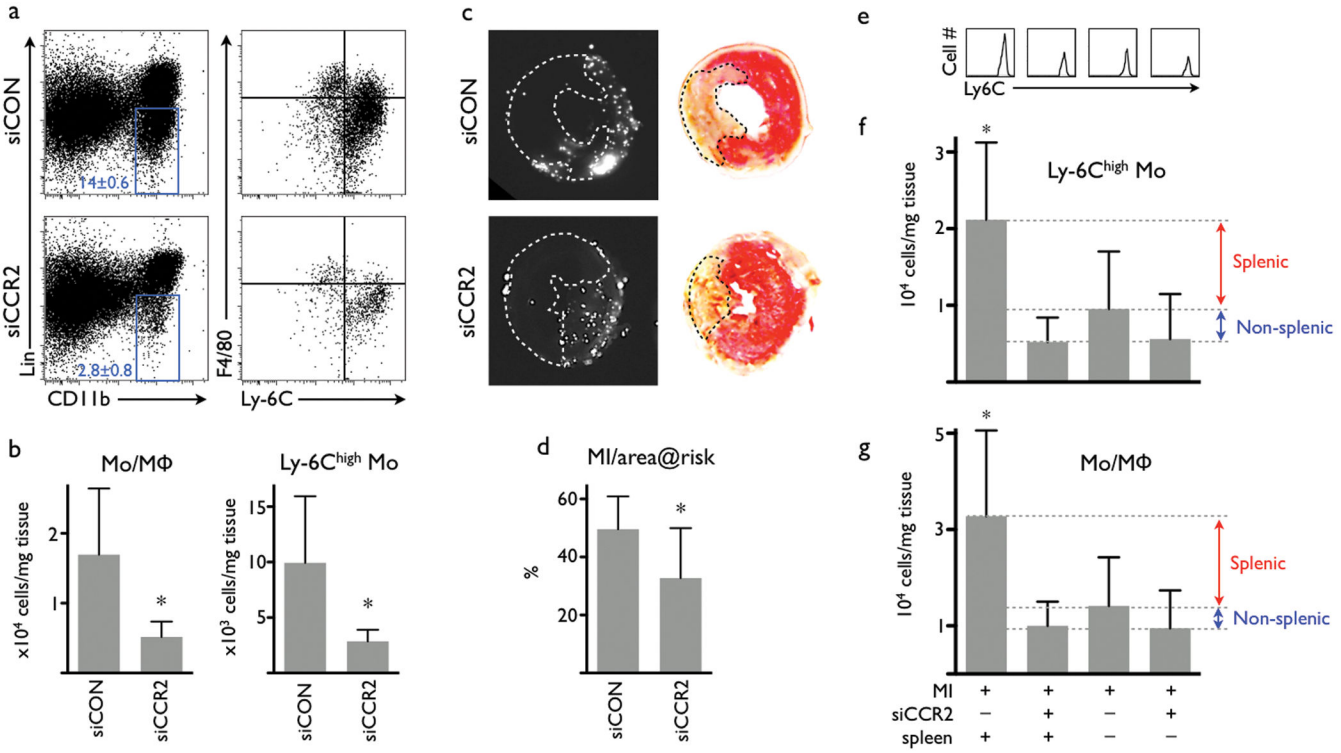

Figure 3. Treatment with siCCR2 reduces ischemia reperfusion injury

(a) FACS of hearts 24 hours after ischemia reperfusion injury (IRI). Dot-plots show a reduction of monocytes/macrophages (blue gate) in the infarct tissue after siCCR2 treatment. Right column of dot plots displays subset analysis with a drastically reduced Ly-6C^{high} monocyte population in the lower right quadrant. (b) Cell tissue numbers for monocytes/macrophages (Mo/MΦ, left) and for Ly-6C^{high} monocytes (n = 9 per group). (c) Fluorescence reflectance images display the area at risk, which is void of microspheres injected during ischemia (left column). TTC staining of the same myocardial short axis slice (right column). The pale, unstained infarct is outlined by a dotted line. (d) Infarct size normalized to the non-perfused area at risk (n = 7-9 per group). (e-f) FACS of infarcts 24 hours after permanent coronary ligation. Spleen “minus” indicates removal of the spleen at time of myocardial infarction. (e) Histogram of Ly-6C^{high} monocytes in infarcts. (f) Number of Ly-6C^{high} monocytes in infarcts. (g) Number of monocytes/macrophages in infarcts. No statistically significant difference was detected between treatment groups (n = 4-8 per group). Mean ± SD, * $P < 0.05$.

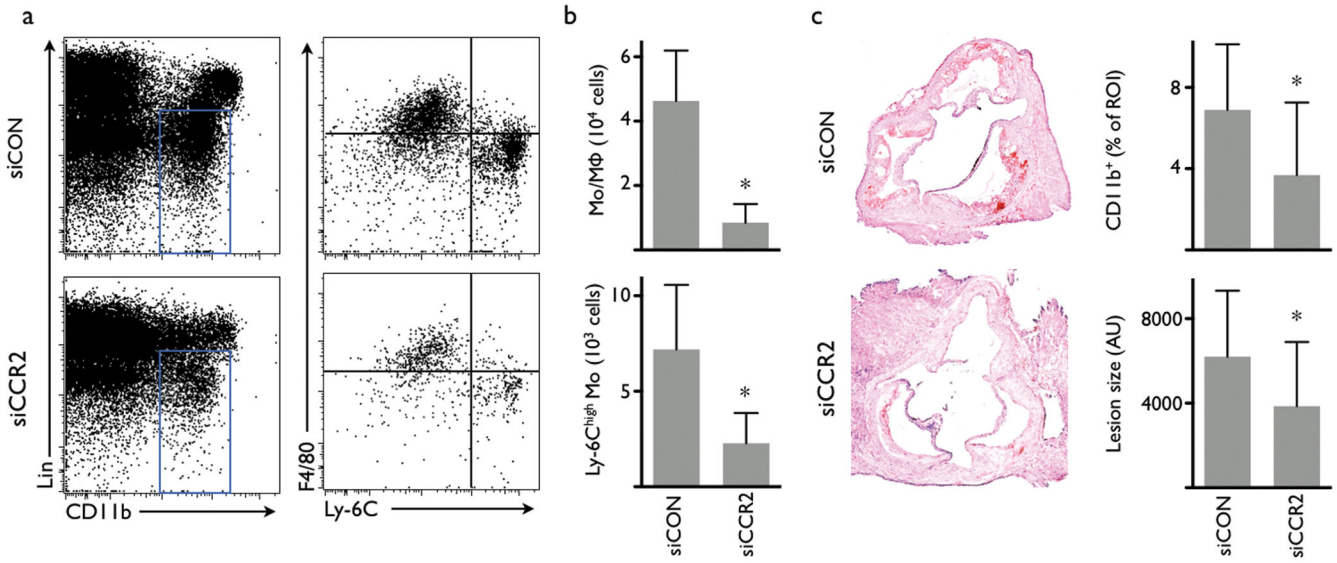

Fig. 4. Treatment with siCCR2 reduces inflammation in atherosclerotic lesions in apoE$^{-/-}$ mice

(a) FACS analysis of cell suspensions retrieved from aortas after 3 weeks of treatment with siRNA targeting CCR2 (siCCR2) or control siRNA treatment (siCON). (b) Number of monocytes and macrophages (Mo/MΦ) and Ly-6C^{high} monocytes in the aortas of apoE$^{-/-}$ mice (n = 10 per group). (c) Immunohistochemical analysis of aortic roots for CD11b and lesion size (n = 8-14 per group). ROI: region of interest. AU: arbitrary units. Mean ± SD, * $P < 0.05$.

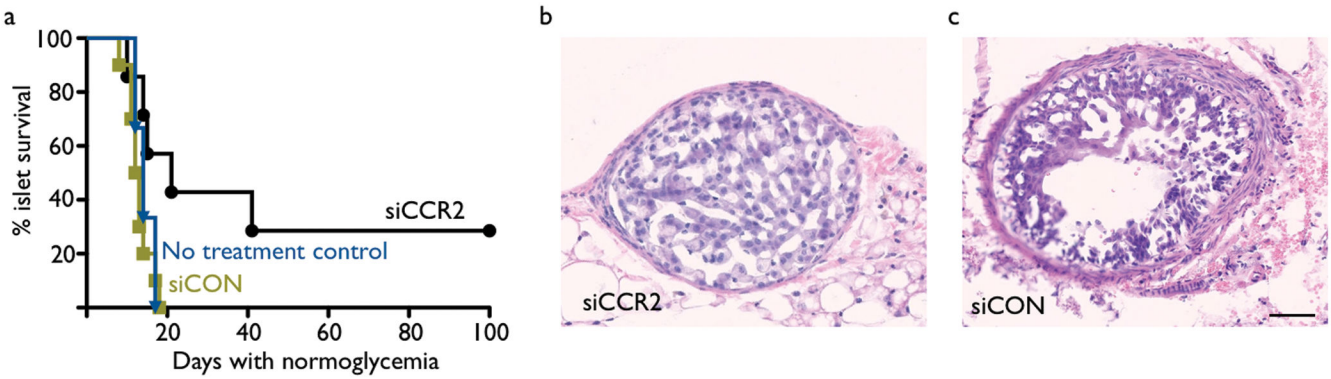

Fig. 5. siCCR2 treatment prolongs survival of pancreatic islet allografts

Diabetic C57/BL/6 mice received BALB/c islets. (a) Survival curve of pancreatic islet transplants in untreated control (blue), siRNA control treated (green) and siCCR2 (black) treated recipients. Rejection was defined as the return of hyperglycemia (blood glucose level >200 mg/dl on two consecutive measurements, n = 7-10 per group). $P < 0.05$. (b) H&E histology of a transplanted islet from a mouse treated with siCCR2. (c) Rejected islet from a control siRNA treated mouse. The scale bar indicates 50μm.

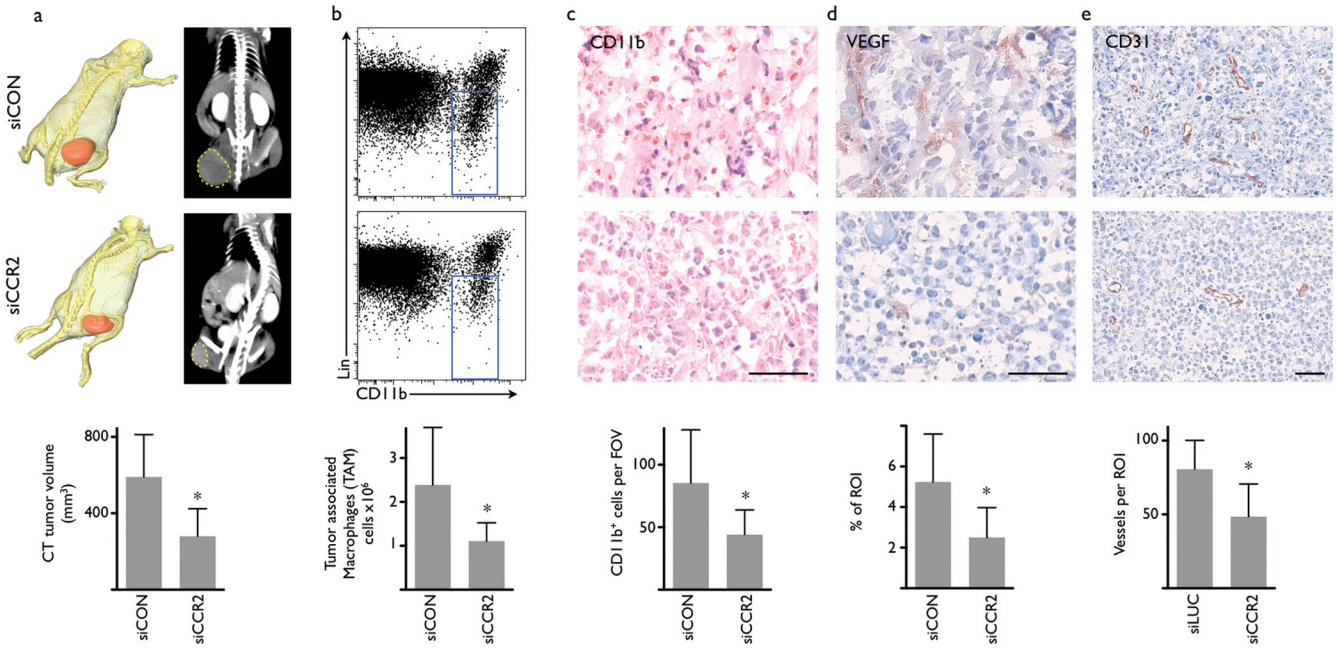

Figure 6. Treatment with siCCR2 reduces tumor size and the number of tumor-associated macrophages (TAM)

(a) Tumor size measured by X-ray CT. Representative images from mice on day 10 after implantation of EL4-tumors (n = 7 per group). Top row displays cohort treated with control siRNA (siCON), bottom row shows siCCR2 treatment. The three-dimensional CT reconstruction shows tumor in red pseudocolor. (b) FACS analysis of tumors with monocyte/macrophage gate (blue) after treatment with control siRNA (top) or siCCR2 (n = 5 per group). (c-e) Immunohistochemical evaluation of tumors for myeloid cells (c, CD11b), vascular endothelial growth factor (d, VEGF) and vessel density (e, CD31). The scale bar indicates 50μm. Mean ± SD, * $P < 0.05$, n = 7 per group.